IDENTIFICATION OF IMPACT CRATERS IN FOILS FROM THE STARDUST INTERSTELLAR DUST COLLECTOR. R. M. Stroud, C. Allen, S. Bajt, H. A. Bechtel, J. Borg, F. Brenker, J. Bridges, D. E. Brownlee, M. Burchell, M. Burghammer, A. L. Butterworth, P. Cloetens, A. M. Davis, C. Floss, G. J. Flynn, D. Frank, Z. Gainsforth, E. Grün, P. R. Heck, J. K. Hillier, P. Hoppe, L. Howard, G. R. Huss, J. Huth, A. Kearsley, A. J. King, B. Lai, J. Leitner, L. Lemelle, H. Leroux, L. R. Nittler, R. C. Ogliore, F. Postberg, M. C. Price, S. A. Sandford, J. A. Sans Tresseras, S. Schmitz, T. Schoonjans, G. Silversmit, A. Simionovici, R. Srama, F. J. Stadermann, T. Stephan, J. Stodolna, S. R. Sutton, R. Toucoulou, M. Trieloff, P. Tsou, A. Tsuchiyama, T. Tyliczszak, B. Vekemans, L. Vincze, A. J. Westphal, M. E. Zolensky, >29,000 Stardust@home dusters. Author affiliations: http://www.ssl.berkeley.edu/~westphal/ISPE/.

Introduction: The Stardust Interstellar Dust Collection tray provides the first opportunity for the direct laboratory-based measurement of contemporary interstellar dust [1]. The total exposed surface of the tray was ~0.1 m^2, including 153 cm^2 of Al foil in addition to the silica aerogel tiles that are the primary collection medium. Preliminary examination of aerogel tiles [2] has already revealed 16 tracks from particle impacts with an orientation consistent with an interstellar origin, and to date four of the particles associated with these tracks have a composition consistent with an extraterrestrial origin. Tentative identification of impact craters on three foil samples was also reported previously [3]. Here we present the definitive identification of 20 impact craters on five foils.

Methods: Preliminary examination of nine foils is currently underway. Foils were first released from the collector tray by use of a rotary cutter, and then mounted on individual stretchers [3]. The stretchers provide mechanical stability for safe shipping and storage, and also serve to flatten the foils for ease in automated imaging.

The primary goal of the first order examination is to provide definitive identification of impact craters, without introducing contamination or otherwise altering the impact residues. Automated imaging of the foils is performed by scanning electron microscopy, using a variety of SEM instruments at several of the home institutions of the team members [4]. The rate of carbon contamination in each instrument, associated with deposition of ambient hydrocarbons under the electron beam, was first assessed according to established protocol [5], to ensure <25 pm of carbon deposition during initial imaging. Low-magnification images of each entire foil surface were obtained at a pixel resolution of 46 to 60 nm/px, depending on the individual instrument. These images were then checked for crater features using a combination of manual observation and automated image analysis routines [6]. Subsequently, identified crater candidates were reimaged individually at three times higher spatial resolution. As a reference for future analysis, the carbon contamination rate during each reimaging session was recorded once or twice on a separate witness plate (clean Al stub), and once per candidate on a crater-free region area within 100 microns of the candidate.

Crater Statistics: First-order imaging of nine foils has been completed (Table 1). Individual imaging of the best identified crater candidates is partially complete for seven foils. The total area scanned for which crater counts are available to-date is 2.74 cm^2, ~2% of the total exposed foil surface. The mean areal density of impact craters is 7±2 cm^{-2}. The crater counts are lower limits; additional craters on these foils may still be identified.

The efficiency of crater detection is expected to vary due to variations in the level of cleanliness and flatness of the foils as well as different analysis techniques (*e.g.*, manual versus automated image analysis). Some foils have considerable coverage with aerogel debris, which can obscure impact features. The variation in flatness of the foils is due to bending during the removal from the collection tray. The stretcher mounts alleviate most, but not all of this variation; and the resultant sample height variation remains a limiting factor for maintaining image focus during automated mapping. Nevertheless, the observed crater densities on the different foils are remarkably consistent, i.e., within 1σ of the mean. The craters are distributed uniformly on the individual foils; no clustering was observed.

Table 1. Areal Density of Impact Craters.

Foil	Area (cm^2)	# of Craters	Crater Density (cm^{-2})
I1061N,1	~0.76	6	5-13[1]
I1032N,1	~0.76	4	2.6-9[1]
I1044N,1	~0.50	4	4-19[1]
I1033N,1	~0.25	2	4-26[1]
I1092W,1	~0.18	2	3-19[1]
I1047W,1	~0.17	0	<22[2]
I1077W,1	~0.12	2	6-38[1]
I1032W,1	~0.30	pending	
I1047N,1	~0.76	pending	

[1] 1 σ confidence range

[2] 2 σ Poisson upper limit

Both circular and ellipsoidal craters have been identified (Fig. 1), ranging in equivalent diameter from 235 nm to 1950 nm (Fig. 2). Some appear to contain visible impact residue (Fig. 1b), and at least one has a dark halo (Fig. 1d), similar to those observed around craters on the Stardust cometary foils, produced by carbonaceous or volatile-rich impactors.

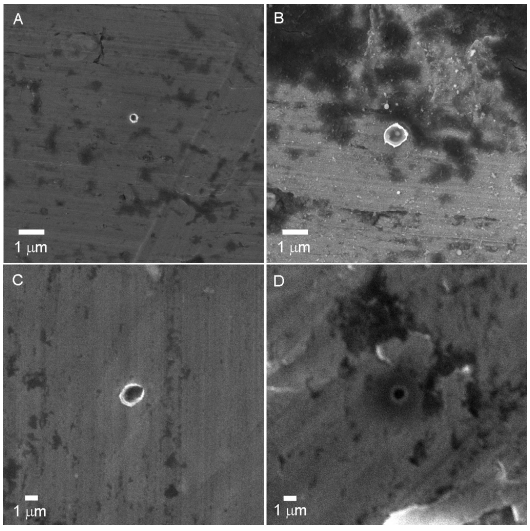

Figure 1. SEM images of impact craters on interstellar foils.

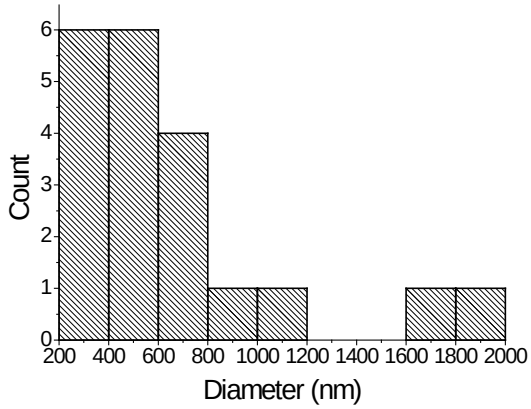

Figure 2. Size distribution of craters as function of equivalent diameter.

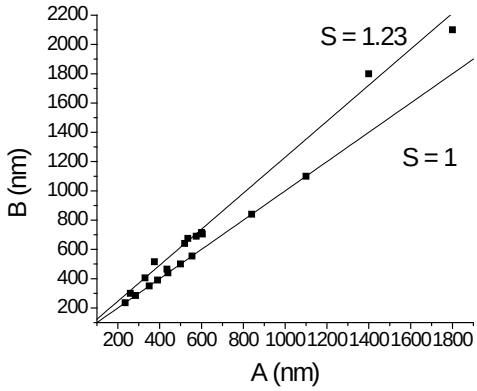

Figure 3. Eccentricity of craters.

The distribution of crater shapes (Fig. 3) suggests two distinct populations, one circular and one with an eccentricity of ~ 1.23. However, this split may be an artifact of the measurement resolution and statistics. Additional data for larger craters, or higher resolution imaging and more rigorous fitting of the crater shapes should clarify this issue in the future.

Discussion: Although we have positively identified impact craters on the Stardust Interstellar foils, the origin of the individual impactors is not yet known. The size distribution of impacting dust required to reproduce the observed crater size distribution is approximately 40 nm to 320 nm, assuming silica spheres with an impact velocity of 20 km/s [7]. In addition to true interstellar dust (ISD) particles, impacts in the observed size range may also result from spacecraft debris and interplanetary nanoscale dust accelerated by the solar wind [8]. Model calculations of ISD trajectories indicate that sub-micron ISD particles with a high charge-to-mass ratio are deflected by the interplanetary magnetic field, and do not reach the inner solar system. Based on these models, the predicted total number of craters due to ISD on the entire foil surface is <20 [9]. However, by extrapolation from the 7 cm^{-2} found on 2% of the foil surface imaged so far, we estimate ~1000 total craters. That approximately 80% of the detected tracks in the aerogel tiles have trajectories indicative of secondary impacts, suggests that a large fraction of the craters are also from secondary events. However, all of the tracks observed to date are from particles >1 μm, whereas all of the craters are from particles <1μm. Thus, direct comparison is difficult because of the complementary nature of the size sensitivity of the imaging of the two collection media. The next phase of the preliminary examination will focus on development of non-destructive methods for determination of the origin of the craters.

References: [1] Brownlee D. E. et al. (2006) *Science* **314**, 1711. [2] Westphal A. et al. (2008) *LPS XXXIX*, #1855; Westphal A. et al. (2011) *LPS XLII*, *this proceedings*. [3] Kearsley A. T. et al. (2010) *MAPS* **73** #5237. [4] Floss C. et al. (2011) *LPS XLII*, *this proceedings*; Leitner J. et al. (2010) *MAPS* **73** #5292; Stroud R. et al. (2010) *MAPS* **73** #5271. [5] Kearsley A. et al. (2010) *LPS XLI* #1593. [6] Ogliore R. et al. *MAPS* **73** #5152. [7] Price M. C. et al. (2010) *MAPS*, in press. [8] Mann I. (2010) *Annu. Rev. Astro. Astrophys.* **48**, 173-203. [9] Landgraf M. et al. (1999) *Planet. Space Sci.*, **47** 1029-1050.